J. of Fire Prot. Engr., 7 (4), 1995, pp 125-132

MODELING THE THERMAL BEHAVIOR OF CONCRETE SLABS SUBJECTED TO THE ASTM E119 STANDARD FIRE CONDITION

Gamal N. Ahmed and James P. Hurst
Portland Cement Association
Skokie, IL

SUMMARY

A mathematical and computational model simulating the coupled heat and mass transfer and related processes in porous media exposed to elevated temperatures has been developed. Taking into account the conservation of mass, momentum, and energy, and the evaporation of free and chemically bound water released by dehydration and their effect on the transport phenomena, a set of three coupled nonlinear differential equations is obtained. Carbonate aggregate concrete slabs subjected to the ASTM E119 standard fire exposure are modeled and validated against test data. Output depicts the coupled relationships between the material's temperature, moisture content, and pore pressure histories and distributions.

INTRODUCTION

Concrete is a porous medium made of cement, water, and aggregate. Under ambient temperature conditions, part of the water is chemically bonded to the cement, while the remainder is contained in the concrete pores as free water. When subjected to sufficient heat, the water evaporates, causing pore pressure to build up. The combined effect of temperature, pore pressure, and mass concentration gradients results in the transport of water vapor and the gaseous mixture of air and water vapor through the material pores. The heat absorbing capabilities of the continuing evaporation/dehydration processes that occur, largely account for the inherent fire resistive properties of concrete.

Pioneer work related to the analytical study of heat and mass transfer in porous media dates back to 1962 with Luikov proposing a mathematical model for representing the coupling of heat and mass transfer[1]. More sophisticated models for computer use were subsequently developed to include the evaporation of physically adsorbed (free) water, and the transport of vapor in the pores. Harmathy[2] proposed a model of simultaneous heat and mass transfer, and predicted the drying process of brick. Similar models have been developed and applied to concrete. An extended literature review is included in the study by Ahmed and Huang[3]. Later generation models to study the coupled heat and mass transfer in concrete at high temperature, taking into account the desorption of physically adsorbed water, plus the decomposition of chemically bound water, are reported by Bazant[4] and others.

The model described herein examines the coupled heat and mass transfer through concrete, by considering the dehydration process of a heated material and the effect it has on the material's pore size and mass transport mechanism. Conservation of mass, momentum, and energy equations, coupled to appropriate constitutive relationships for the material, have led to the current mathematical and computational model which is capable of adding important knowledge to the art of behavior of porous materials at elevated temperatures. Various initial and boundary conditions, *i.e.*, moisture

content, other material properties, assembly geometries, and specified heat source can be considered by the model for any porous material.

The model can be used for both research and design purposes. From a research standpoint, the following can be investigated: (1) spalling potential based on pore pressure and temperature at a given concrete depth; (2) the influence of material properties (moisture content, permeability, porosity, etc.) on the fire performance of concrete through the use of parametric studies; and (3) the effect of various specified fire exposures on the performance of concrete. For design purposes, the model can be used as follows: (1) to calculate fire resistance ratings of barrier assemblies such as walls and floor/ceilings (based on the ASTM E119 heat transmission criterion); (2) to optimize concrete and masonry geometries with respect to retarding heat transmission; (3) as a tool to support findings from field inspections of fire-damaged concrete; and (4) to provide temperature distribution information that can be used in structural analytical methods for predicting structural fire performance. The model is mainly self-driven, as it does not require a lot of user input or assumptions. Numerical and graphical results can be obtained using readily available PC hardware.

Research Significance

Fire resistance ratings of concrete slabs (walls and floors) are typically based on the average heat transmission criterion specified in various fire test standards. In North America, where the governing standard is ASTM E119, this means that an average temperature increase of 139 °C (250 °F) on the specimen's unexposed surface will occur, prior to the time of the specimen's structural failure (assuming adequate concrete cover protection to the reinforcing steel is provided). As a result, structural considerations can often be neglected for purposes of determining fire endurance of concrete slabs.

This paper presents the use of a computer model to analyze the thermal response of carbonate aggregate concrete slabs subjected to the ASTM E119 standard fire exposure.[5] Computer output consisting of the unexposed surface temperatures of various reference slabs is compared to the average unexposed surface temperatures of corresponding specimens from laboratory testing. Output from the model will also reveal the dependent relationships that exist between temperature, moisture content, and pore pressure within a given depth of concrete slab thickness. Structural performance is not considered by the model. However, it does provide results for evaluation of the concrete's spalling potential based on the material's pore pressure build-up and temperature distribution.

Model Description

Heat and Mass Transfer Phenomena

Concrete contains fine pores that are occupied by adsorbed water, air, and water vapor. Water vapor is in equilibrium with the adsorbed water. When concrete is intensely heated during fire, the free water undergoes evaporation and diffusion, and a gaseous mixture of water vapor and air is transported through the concrete pores by convection. As the material temperature increases, the chemically bound water contained in the cement paste is released into the pores by dehydration, and evaporates. The transmission of heat through the concrete is thereby retarded as a result of the energy absorbed in the dehydration and evaporation processes. This process continues until the material is totally dehydrated. The mass transport (gaseous phase) through the concrete contributes to the heat transfer and influences the material's temperature profile. All of these phenomena are considered by the model.

Assumptions and Considerations

Assumptions and considerations are included as follows: concrete is a multiphase porous system, considered as a continuous medium. Local thermodynamic equilibrium

is assumed. The mobility of liquid is negligible compared to that of the gaseous mixture. Water vapor, air, and their gaseous mixture follow the universal ideal gas law. Saturation vapor pressure of free water is assumed to be given by the Clausius-Clapeyron equation. The local equilibrium moisture content is related to the relative vapor pressure and temperature in concrete according to $w = w(P^o_v / P_v, T)$. This constitutive relation is expressed as a set of sorption isotherms. The thermal decomposition of chemically bound water is considered and determined by thermogravimetric analysis. Physical and thermal properties (thermal conductivity, heat capacity, permeability, etc.) are strongly dependent on temperature, pore pressure, and moisture content. Evaporation/condensation mechanisms for water contained in concrete pores are taken into account. Conductive heat, and convective and diffusive mass and heat transfer through the porous medium are considered. Convective heat and mass transfer are driven by pore pressure gradients; diffusive transport is driven by mass concentration gradients; and conductive heat transfer is driven by temperature gradients.

Governing Equations

Conductive heat transfer within the gaseous mixture (water vapor and air) driven by temperature gradient is assumed to conform to Fourier's law, $q = -\varepsilon_g k_g (\partial T / \partial x)$. Diffusion of water vapor within the gaseous mixture driven by the concentration gradient is assumed to conform to Fick's law, $J = -\rho_g \varepsilon_g D(\partial \varphi / \partial x)$. Convective mass transport of gaseous mixture driven by pore pressure gradient is assumed to conform to Darcy's law, $V_g = -(K_g / g\rho_g)(\partial P / \partial x)$.

The conservation of mass equations for liquid water, water vapor, and the gaseous mixture of water vapor and air in the one-dimensional form are:

$$\frac{\partial \delta l}{\partial t} = -\Gamma \tag{1}$$

$$\frac{\partial}{\partial t}(\rho_v \varepsilon_g \varphi) + \frac{\partial}{\partial x}(\rho_v \varepsilon_g V_g \varphi) - \frac{\partial}{\partial x}\left(\rho_g \varepsilon_g D \frac{\partial \varphi}{\partial x}\right) = \Gamma \tag{2}$$

$$\frac{\partial}{\partial t}(\rho_g \varepsilon_g) + \frac{\partial}{\partial x}(\rho_g \varepsilon_g V_g) = \Gamma \tag{3}$$

The mass concentration of liquid water per unit volume of porous medium is defined as:

$$\delta_l = \delta_{lf} + \delta_{ld} \tag{4}$$

The mass concentration per unit volume of porous medium of free water, δ_{lf}, and chemically bound water released into the pores by dehydration, δ_{ld}, are defined, respectively, as:

$$\delta_{lf} = \rho_l (\varepsilon - \varepsilon_g) \tag{5}$$

$$\delta_{ld} = \left(\frac{\rho - \rho_e}{\rho_o - \rho_e}\right)\delta_{ldo} \tag{6}$$

Where: $\delta_{ldo} = \rho_o - \rho_e$ (7)

$$\varepsilon = \left(\varepsilon_o + \frac{\delta_{ldo} - \delta_{ld}}{\rho_l}\right)\left(1 + 0.12\left(\frac{P_v}{P^o_v} - 1.04\right)\right),$$

$$\text{for } \frac{P_v}{P^o_v} \geq 1.04 \tag{8}$$

$$\text{or: } \varepsilon = \varepsilon_v + \left(\frac{\delta_{ldo} - \delta_{ld}}{\rho_l}\right) \text{ for } \frac{P_v}{P^o_v} < 1.04 \tag{9}$$

The conservation of energy equation in one dimension can be given as:

$$\rho C_p \frac{\partial T}{\partial t} + \rho_g \varepsilon_g C_{pg} V_g \frac{\partial T}{\partial x} - \left(\rho_g \varepsilon_g (C_{pv} - C_{pa}) D \frac{\partial \varphi}{\partial x} \right) \frac{\partial T}{\partial x} = \frac{\partial}{\partial x} \left(k \frac{\partial T}{\partial x} \right) - Q\Gamma \quad (10)$$

The effective heat capacity of the transient energy term, ρC_p, is defined as:

$$\rho C_p = (1-\varepsilon)\rho_s C_{ps} + (\varepsilon - \varepsilon_g)\rho_l C_{pl} + \varphi \varepsilon_g \rho_v C_{pv} + (1-\varphi)\varepsilon_g \rho_a C_{pa} \quad (11)$$

The effective thermal conductivity of the conductive energy term, k, is defined as:

$$K = \left((1-\varepsilon) k_s^{1/4} + (\varepsilon - \varepsilon_g) k_l^{1/4} + \varepsilon_g k_g^{1/4} \right)^4 \quad (12)$$

The evaporation/dehydration term in energy equation, $Q\Gamma$, is defined as:

$$Q\Gamma = -\left(Q_l \frac{\partial \delta_{lf}}{\partial t} + Q_{dhev} \frac{\partial \delta_{ld}}{\partial t} \right) \quad (13)$$

$$Q_{dhev} = Q_l + Q_{dh} \quad (14)$$

Initial and Boundary Conditions

The initial conditions are given by the uniform distribution of temperature, pore pressure, and moisture content in the concrete at reference time zero. The boundary conditions simulate concrete slabs exposed to fire from one side and ambient conditions on the other side. The boundary conditions for the conservation of energy equation are specified as the convective and radiative heat exchange at the surfaces of the concrete slabs with variable convective and radiative heat transfer coefficients. Since the pressure along the boundaries is considered to be atmospheric, the mass flow at all boundaries is specified as diffusive mass flow with variable mass transfer coefficients.

Given the specified assumptions and considerations, and making use of the concepts of continuum mechanics, principles of irreversible thermodynamics, and conservation of mass, momentum, and energy equations coupled to constitutive relationships for the material, a set of three coupled, nonlinear, and second-order partial differential equations is obtained. This system of equations, coupled with nonlinear boundary conditions, can only be solved using numerical techniques.

Numerical Method

This method utilizes a fully implicit finite difference scheme, incorporating quasi-linearization of the nonlinear coefficients and the mixed derivatives. Coupling the discretized boundary conditions with the linearized set of implicit finite difference equations results in a three-by-three block system of equations[6]. Using algebraic manipulation, this system of equations is converted into a three-by-three block tridiagonal system, which is solved using a block-tridiagonal solver routine developed for this purpose. Variable grid spacing is used to reduce or eliminate the potential of pore pressure fluctuations from occurring. Use of variable time steps minimizes the computing time and reduces the effect of truncation errors.

Results and Discussion

In the examples that follow, the effect of the coupled heat and mass transfer and related phenomena in heated concrete is investigated through computer analysis of the material's moisture content, temperature, and pore pressure histories and distributions. All of the figures pertain to carbonate aggregate concrete slabs subjected to the ASTM E119 time-temperature condition. Figures 1 and 2 are used for validating the model. Figure 1 compares ASTM E119 test results for the average unexposed surface temperature of various thickness concrete slab specimens, with results predicted by the model. Figure 2 compares laboratory measured tem-

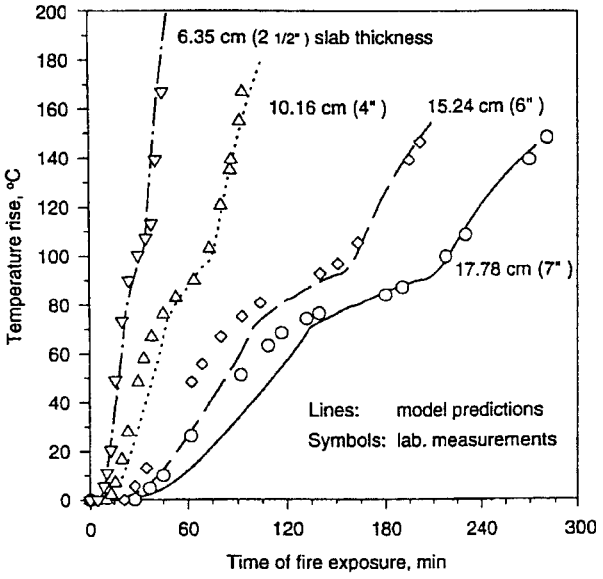

Figure 1. Comparison of the E119 Measured Average Unexposed Surface Temperatures of Concrete Slabs against Those Predicted by Computer Modeling.

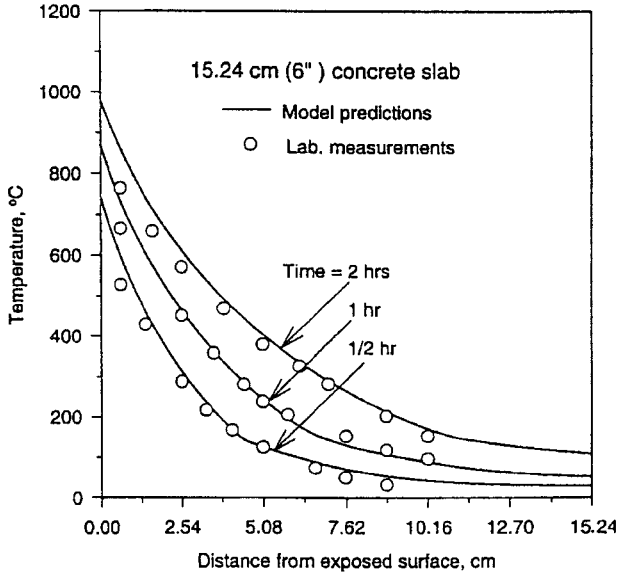

Figure 2. Comparison of the Predicted Temperature Distribution in a 15.24 cm (6") Concrete Slab against E119 Measured Results.

perature distributions within a 15.24 cm (6") slab for various times, against those predicted by the model.

The agreement of the modeled results in Figure 1 with experimental ones reported by Abrams and Gustaferro[7] is very good. This is especially true for the time periods that represent the fire resistance ratings of slab thicknesses based on the E119 average temperature criterion (temperature rise of 139 °C [250 °F]). For reference, these times are as follows: 6.35 cm (2 and 1/2") - 41 minutes; 10.16 cm (4") - 87 minutes; 15.24 cm (6") - 196 minutes; and 17.78 cm (7") - 271 minutes. With respect to Figure 2, there is excellent agreement. Figure 3 provides additional temperature distribution curves from the model, as an extension of those in Figure 2.

Figures 3-8 graphically depict the coupled relationships between the temperature, moisture content, and pore pressure histories and distributions. These figures are used to describe concrete's thermal response to heat.

In the early stages of heating, the temperature rise of the concrete is primarily influenced by conduction and diffusion. At about 100 °C, significant evaporation of the free water begins, and the chemically bound water is released into the pores by dehydration. As evaporation continues, pore pressure develops, and the gaseous mixture of air and water vapor is driven toward the slab surfaces. Some of the mixture exits through the hot surface, while the rest is forced into the cooler zones of

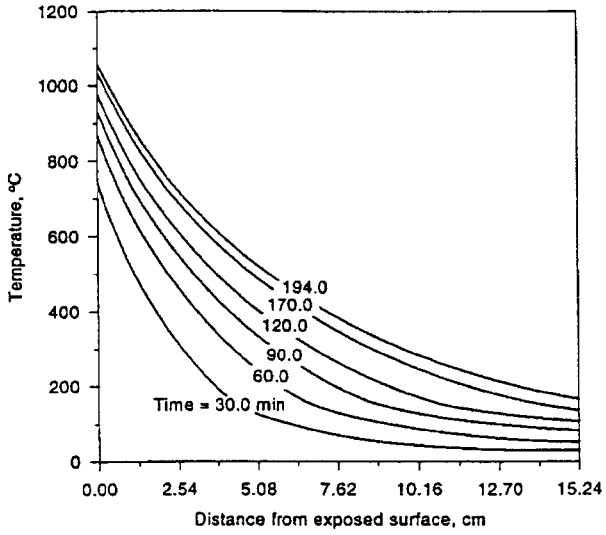

Figure 3. Model-Predicted Temperature Distribution at Various Times for a 15.24 cm (6") Concrete Slab Subjected to the E119 Time-Temperature Condition.

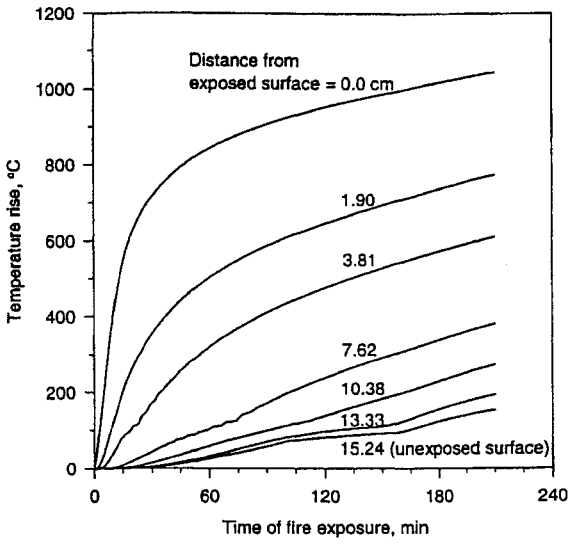

Figure 4. Model-Predicted Temperature History at Different Depths of a 15.24 cm (6") Concrete Slab Subjected to the E119 Time-Temperature Condition.

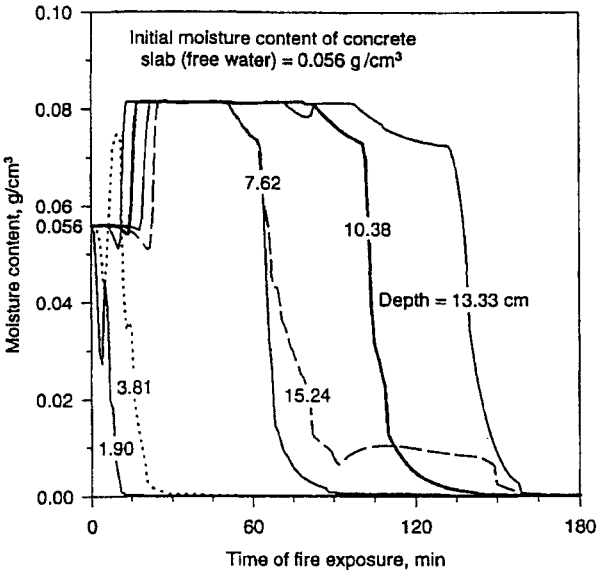

Figure 5. Model-Predicted Moisture Content History at Different Depths of a 15.24 cm (6") Concrete Slab Subjected to the E119 Time-Temperature Condition.

the material, where it condenses and accumulates as liquid. This convective migration of the gaseous mixture and accumulation (moisture clog) in the neighboring zone is shown in Figure 5. The presence of migrated water vapor, as accumulated condensate, is indicated by portions of the curves that are above the level of the initial (free water) moisture content. Corresponding pore pressures at various depths, representing the driving force of the convective transport mechanism, are presented in Figure 7. Low levels of low pore pressure in Figure 7 are the result of low rates of evaporation and indicate that the transport mechanism is due to diffusion rather than convection. If these times and depths are cross-referenced with those in Figure 4, a low evaporation rate is confirmed by temperatures that are less than 100 °C.

After the development of the moisture clog has occurred, the evaporation/dehydration process continues at the drying (evaporation) front. The result is a step-like relationship of increasing temperature, whereby the temperature rise is retarded at regular intervals due to the energy being absorbed during dehydration and/or the change of phase. The curves representing distances of 3.81 and 7.62 cm from the fire-exposed surface in Figure 4 most clearly display this step-like pattern.

Continued evaporation, plus the clog's resistance to convective transport, causes the pore pressure to increase further and force the clog in the direction of the unexposed surface. The pore pressure distribution, shown in Figure 8, effectively tracks

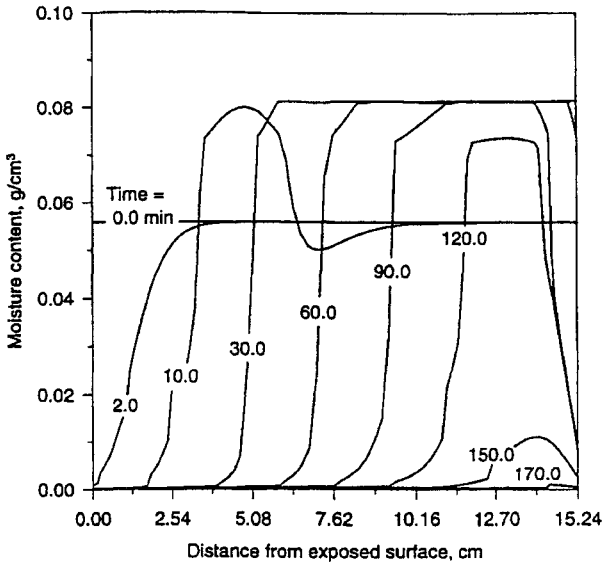

Figure 6. Model-Predicted Moisture Content Distribution at Various Times for a 15.24 cm (6") Slab Subjected to the E119 Time-Temperature Condition.

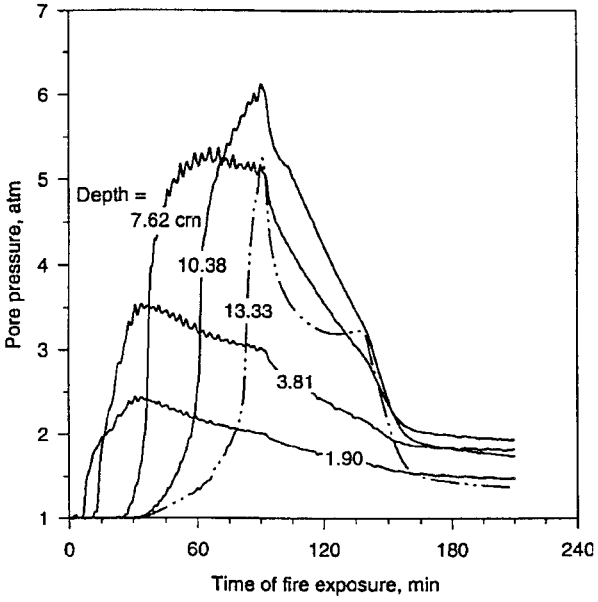

Figure 7. Model-Predicted Pore Pressure History at Different Depths of a 15.24 cm (6") Concrete Slab Subjected to the E119 Time-Temperature Condition.

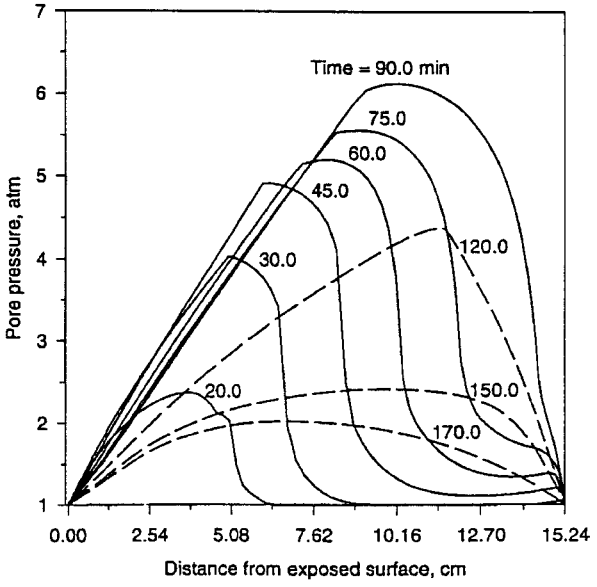

Figure 8. Model-Predicted Pore Pressure Distribution at Various Times for a 15.24 cm (6") Concrete Slab Subjected to the E119 Time-Temperature Condition.

the position of the clog and its movement. Figure 6, describing the moisture content distribution, provides similar information on the clog's position and movement. Note that the maximum pore pressure at a given time and depth in Figure 8 is consistent with the sharp loss of moisture (high evaporation rate) shown in corresponding curves of Figure 6. This is logical, since there is little moisture remaining in the zone vacated by the passing clog. The fact that air remains in the pores after drying, explains why there is a time lag involved in the loss of pressure (see Figures 7 and 8). The behavior described above is repeated until the slab becomes totally dry. With no additional moisture available for evaporation, the pressure in the pores eventually dissipates and returns to atmospheric.

Another important observation that can be made from the figures is the potential of spalling. Figure 7 indicates that the maximum pore pressure occurs at a distance of 10.38 cm from the fire exposed surface. Cross-referencing this to Figure 4 at the time of maximum pore pressure shows that, although the pressure is high, the temperature is low at this depth. Conversely, at depths where high temperatures occur, the pore pressures are low. Neither of these conditions are conducive to spalling. The absence of spalling problems associated with the Abrams and Gustaferro test program[7] supports this premise.

Conclusions

With respect to the model, the following conclusions are offered. The model's prediction of heat and mass transfer through the specimen is in close agreement with laboratory results based on the average heat transmission criterion of the ASTM E119 standard fire test. Good agreement in validating the model for the unexposed surface temperature of the sample specimens, plus the consistencies between moisture content, pore pressure, and temperature histories within the specimen, further validate the coupled heat and mass transfer relationship that exists between moisture content, pore pressure, and temperature. The model can perform complex analyses, for research and design use, involving aspects of material behavior that is not easily obtained or measured by experiment (*i.e.*, moisture content and pore pressure distributions).

Nomenclature

C_p effective specific heat, kJ/kg K

C_{pi} specific heat of i-component, kJ/kg K

D modified diffusity of the gaseous mixture, m^2/s

g gravity acceleration, m/s^2

J molecular mass flux, kg/m^2 s

k effective thermal conductivity, W/m K

k_i thermal conductivity of i-component, W/m K

K_g permeability, m/s

P pore pressure of gaseous mixture, N/m^2

P_v partial pressure of water vapor, N/m^2

P^o_v equilibrium vapor pressure of bulk water, N/m^2

Q_l latent heat of evaporation, kJ/kg

Q_{dh} heat of dehydration of ch. bound water, kJ/kg

Q_{dhev} heat of evaporation and dehydration, kJ/kg

R universal gas constant, kJ/kmol K

t time, s

T absolute temperature, K

V_g velocity of gaseous mixture, m/s

x space coordinate, m

δ_i mass concentration of i-component per unit volume of porous medium, kg/m^3

δ_{ld} chemically bound water content, kg/m^3

$(\delta_{ldo}-\delta_{ld})$ chemically bound water released into pores by dehydration, kg/m^3

δ_{lf} free water content in pores, kg/m^3

ε porosity of porous medium, m^3/m^3

ε_g volume fraction of gaseous mixture in porous medium, m^3/m^3

Γ mass rate of evaporation per unit volume of porous medium, kg/m^3 s

φ mole fraction of water vapor of gaseous mixture, kmol/kmol

ρ effective density of porous medium, kg/m^3

ρ_i density of i-component, kg/m^3

ρC_p heat capacity of porous medium, kJ/m^3K

Subscripts

a air of gaseous mixture

d dry porous medium

e end of dehydration process of porous medium

g gaseous mixture

i i-component (a-, g-, l-, s-, v-component) of porous medium

l liquid phase

o initial condition or datum

s solid phase

v water vapor

REFERENCES

1. Luikov, A. V., *Heat and Mass Transfer in Capillary-Porous Bodies*, Pergamon, Oxford, 1966.

2. Harmathy, T. Z., Simultaneous Moisture and Heat Transfer in Porous Systems with Particular Reference to Drying, *I & E C Fundamentals*, Vol. **8**, No. 1, 1969.

3. Ahmed, G. N. and Huang, C. L., "Modeling of Concrete Slabs under Fire," Chemical Engineering Communications, *International Journal of Chemical Engineering*, Vol. **91**, 1990, pp. 241-253.

4. Bazant, Z. P. and Thonguthai, W., "Pore Pressure in Heated Concrete Walls-Theoretical Prediction," *Magazine of Concrete Research*, Vol. **31**, No. 107, 1979, pp. 67-76.

5. ASTM Designation E 119-88, *Standard Methods of Fire Tests of Building Construction and Materials*, Section 4, Vol. **04.07**, American Society for Testing and Materials, Philadelphia, PA, 1994.

6. Huang, C. L. and Ahmed, G. N., "Influence of Slab Thickness on Responses of Concrete Walls under Fire," Numerical Heat Transfer, *International Journal of Computation and Methodology*, Part A: Applications, Vol. **19**, No. 1, 1991, pp. 43-64.

7. Abrams, M. S. and Gustaferro, A. H., "Fire Endurance of Concrete Slabs as Influenced by Thickness, Aggregate Type, and Moisture," *Research Department Bulletin* 223, PCA, 1968.